Journal of Power Sources 193 (2009) 80–85

Contents lists available at ScienceDirect

Journal of Power Sources

journal homepage: www.elsevier.com/locate/jpowsour

Effect of Al and Ce doping on the deformation upon sintering in sequential tape cast layers for solid oxide fuel cells

M. Cologna [a,b,*], A.R. Contino [a], D. Montinaro [c], V.M. Sglavo [a,b]

[a] DIMTI, Università degli Studi di Trento, via Mesiano 77, I-38050 Trento, Italy
[b] INSTM, Trento Research Unit, via G. Giusti 9, 50121 Firenze, Italy
[c] SOFCpower S.r.l., via Trento 117, 38017 Mezzolombardo (TN), Italy

ARTICLE INFO

Article history:
Received 10 October 2008
Received in revised form 8 December 2008
Accepted 9 December 2008
Available online 24 December 2008

Keywords:
Solid oxide fuel cells
Co-sintering
Curvature
Dopant
Anode
Tape casting

ABSTRACT

Water-based tape casting is an attractive production route for planar solid oxide fuel cells (SOFCs) due to its high productivity and reduced environmental issues. In this work planar anode supported SOFCs with thin electrolyte were prepared by water-based sequential tape casting and co-sintering. An in situ high temperature monitoring apparatus was assembled to allow the determination of free sintering shrinkage of thin green tape cast layers and to follow the curvature developed in multilayers during the entire sintering process.

The instantaneous curvature developed upon co-sintering was studied as a function of the firing schedule and layer composition. It was found that by tailoring the electrode composition it is possible to reduce the shrinking rate difference between anode and electrolyte thus obtaining defect-free electrolyte, minimising the residual curvature of the half-cell and improving the electrochemical performances of the cell.

1. Introduction

Planar anode supported solid oxide fuel cells are ceramic devices constituted of stacked layers of different materials with dissimilar physical and mechanical properties. The fabrication of such devices typically requires the multi-step deposition and successive firing of the different layers. The cost of such high temperature treatments represents a significant fraction of the overall production expenses. In order to maintain the SOFC costs to an acceptable level, the production of the anode and electrolyte precursor layers by relatively cheap powder technologies, like tape casting or screen printing and subsequent one-step co-sintering, is the preferred route.

In general, during co-sintering of multilayered ceramics, stresses are generated due to the mismatch in thermal expansion coefficient and different sintering rate [1–4]. The stresses generated by dissimilar sintering rates are the primary cause of the deformation of the cell, specifically a curvature, which is developed upon co-firing; and if such stresses overcome the intrinsic strength of the layers, they can lead to flaws and defects formation. Co-sintering is a particularly delicate issue in SOFC processing: the anode needs to sinter in order to acquire enough mechanical strength to support the cell but needs to preserve sufficient porosity for fuel flow; conversely, the thin electrolyte acting as the gas separator between fuel and oxygen needs to densify at least to a point where it retains non-interconnected porosity only. As a matter of fact, SOFC are not tolerant to the presence of defects and even a small crack in the electrolyte leads to leakage and hot spots associated to direct combustion that decreases electrochemical performances and accelerates degradation. Moreover, any defect is detrimental for SOFC mechanical properties, which are of utmost importance in the real operation of a stack even for stationary applications, where the cells can be subjected to severe stresses deriving from external applied load or from thermal or RedOx cycles. Many efforts are being currently done in order to reduce the curvature development and flaws generation, by varying the starting powder grain size [5,6], through selective coarsening of NiO or YSZ powder [7,8] or by optimising the electrodes sintering [9] or co-sintering temperature [10].

Yttria (8 mol%) stabilised zirconia (YSZ) for the electrolyte and a mixture of YSZ and Ni are by far the most studied and employed compositions in SOFC production [7,11–13]. Although such well-known materials are the mayor constituents of anode supported half cells, a variety of doping elements are usually added in small quantities in both the anode and the electrolyte in order to enhance mechanical properties, electrochemical performances, long-term stability and resistance to RedOx cycles. For example, the addition of small quantities of Al_2O_3 (in the order of 1%) to cubic YSZ has been reported to act as sintering aid [14,15] which enhances hardness and fracture toughness, reduces grain growth in YSZ electrolyte [16]

* Corresponding author at: DIMTI, Università degli Studi di Trento, via Mesiano 77, I-38050 Trento, Italy. Tel.: +39 0461881922; fax: +39 0461881945.
E-mail address: marco.cologna@ing.unitn.it (M. Cologna).

0378-7753/$ – see front matter © 2008 Elsevier B.V. All rights reserved.
doi:10.1016/j.jpowsour.2008.12.052

Table 1
Composition of electrolyte and anode slurry (vol.%)[a].

Components	Electrolyte	Anode
Powder	28.4	21.3
Dispersant	1.5	2.8
Water	58.2	53.0
Binder	11.9	22.9

[a] Binder and dispersant are reported on dry basis.

and significantly increases flexural strength of NiO/YSZ anode [17]. Oxides like Cr_2O_3, TiO_2, Al_2O_3, and Sc_2O_3 can improve anode RedOx stability [18]. Addition of small quantities of Mo [19], precious metals like Ru and Pt [20] or CeO_2 [21] has been observed to reduce the carbon deposition on Ni/YSZ anode during methane reforming. The use of CeO_2 has also been shown to improve the electrochemical performance of Ni/YSZ anodes [22].

Despite the importance and the widespread use of reactive elements and sintering aids and the delicate issue of co-firing for the successful production of reliable cells, no specific studies have been carried out addressing the effect of doping elements on the anode sintering rate and, consequently, on the transient stresses developed upon co-sintering with the electrolyte, which are the primary cause for cell curvature and defect formation. The aim of the present work is to study the effect of selected doping substances (like Al_2O_3 or CeO_2) on the anode sintering kinetics and, consequently, on the cell curvature and curvature rate; in addition it is aimed to determine whether the addition of doping elements can be successfully employed to reduce defects development upon sintering and residual curvature, with the ultimate goal of obtaining flat and higher quality cells.

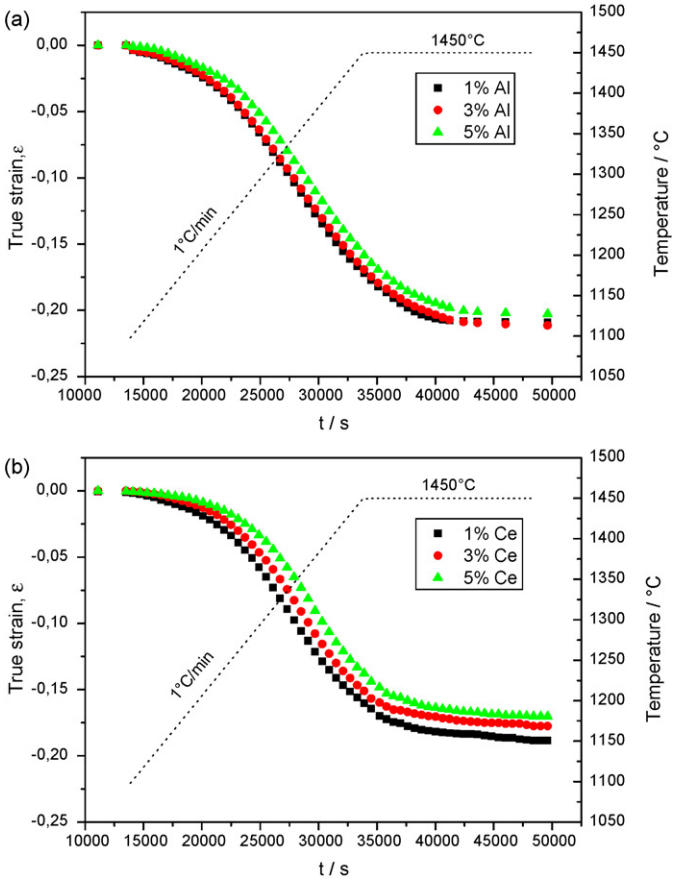

Fig. 1. True strain as a function of time for (a) Al- and (b) Ce-doped pressed pellets.

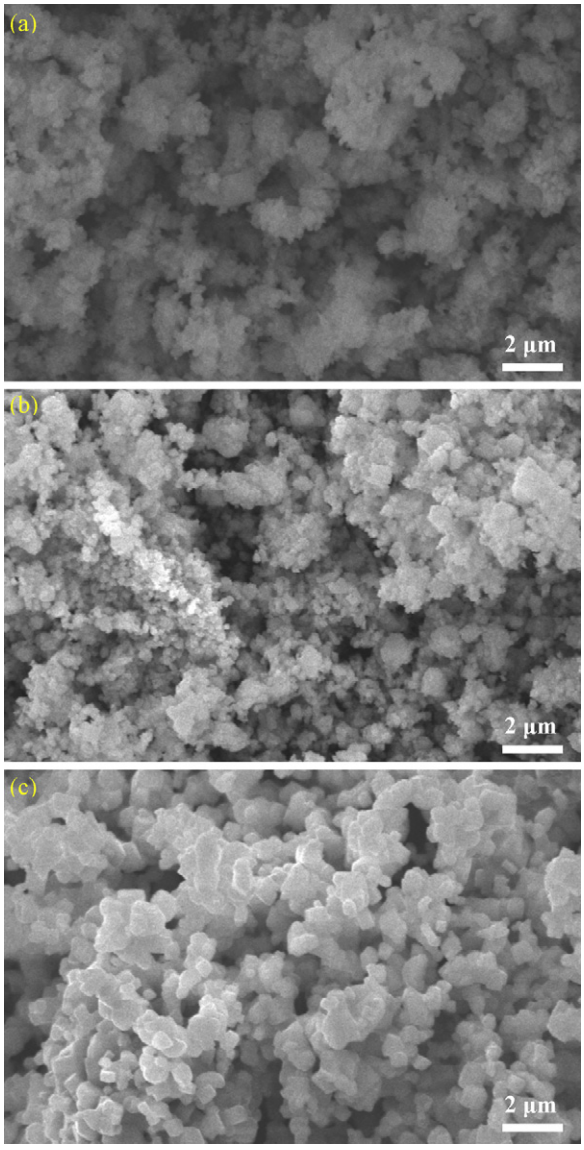

Fig. 2. Micrographs of the modified NiO powders. 1 mol% Al-doped (a), 5 mol% Ce-doped (b) and simply calcined (c).

2. Materials and methods

Due to their wide use as doping elements for typical SOFC anode, Al and Ce were selected in the present work. NiO powder with 1, 3 and 5 mol% Al or Ce doping agent was produced by adding $Al(NO_3)_3{\cdot}9H_2O$ (Riedel-De Haen, Germany) or $Ce(NO_3)_3{\cdot}6H_2O$ (Alfa Aesar, Germany) to starting NiO powder (J.T. Baker, USA) in a plastic jar containing ethanol and zirconia balls (Inframat Advanced Materials, USA); the mixture was milled for 18 h. The powders were then dried and calcined for 10 h at 900 °C. Pure NiO powder was also calcined for 10 h at 900 °C for comparison. Specific surface area (SSA) was determined by nitrogen adsorption (BET) method (ASAP 2010, Micromeritics, USA). Doped NiO powder was mixed with 8 mol% yttria stabilised zirconia (YSZ) powder (TZ-8YS, SSA 6 $m^2\ g^{-1}$, Tosoh, Japan) in a ratio 58 wt% NiO and 42 wt% YSZ; binder (B1000, Duramax, Rohm and Haas, France) and distilled water were then added and the blend was mixed for 5 h in a rotating plastic drum containing zirconia balls. The powders were then dried and manually ground in a mortar. A portion of the obtained powder was then pressed at 125 MPa for 120 s into 20 mm diameter/1 mm thickness pellets that were used for preliminary sintering analyses.

Anode and electrolyte were prepared by water-based tape casting technology. YSZ powder was used for the electrolyte; a mixture of 58 wt% NiO and 42 wt% YSZ powder was selected for the anode. NiO powder was screened through a 100 μm sieve, mixed with YSZ powder, water and dispersant (Darvan 821A, R.T. Vanderbilt Inc., USA) in a plastic drum containing zirconia balls. The electrolyte suspension was milled for 3 h in a Turbula mixer (Bachofen, Switzerland); conversely, the anode was mixed for 18 h in a conventional rotator mill. After de-gassing, binders were added (B1000 and B1014, Duramax, Rohm and Haas, France) and the mixtures were mechanically stirred for 2 h. Slurries composition is reported in Table 1. Green half cells were produced by casting the anode slurry on the top of the previously cast and dried electrolyte in a laboratory-scale tape casting equipment. The green electrolyte and anode thickness was 22 ± 2 and 420 ± 10 μm, respectively. The green bi-layers were cut into rectangular bars of approximately 10 mm length and 1 mm width for curvature observation; conversely, monolithic tapes were cut into bars of approximately 20 mm length and 5 mm width for shrinkage measurement. The samples were then sintered in a tubular furnace (HTRH 100-300/18, GERO Hochtemperaturöfen GmbH, Germany) at 1450 °C for 4 h using a heating rate of 1 °C min^{-1}.

Shrinkage and curvature evolution upon sintering were determined with a CCD camera acquiring pictures at regular intervals through a series of optical filters. Images were processed with the freeware software ImageJ 1.38 J.

The microstructure of the materials was analyzed by scanning electron microscope (SEM, JSM 5500, JEOL, Japan).

A thin cathode (50 μm thick) was deposited by screen printing an ink containing equal weight of lanthanum strontium manganite and YSZ powders ($La_{0.65}Sr_{0.35}MnO_3$—SSA 9.3 m^2 g^{-1}, YSZ—SSA 13 m^2 g^{-1}, Nextech Materials, USA) on selected samples (active area = 1.9 cm^2). Electrochemical tests were performed using specifically developed test bench for single-cell configuration [23] in order to evaluate the cells performance. Measurements were performed at 800 °C; 150N ml min^{-1} of 97% H_2–3% H_2O gas mixture and 300N ml min^{-1} of air were flown to the anode and the cathode, respectively.

3. Results and discussion

A first evaluation of the effect of the dopant addition on sintering behaviour of NiO/YSZ based anodes was performed on the pellets produced by pressing and sintering. It is well known that differences in the starting density in otherwise identical powder compacts lead to different sintering rates [24]; therefore, the initial bulk density of the pellets was evaluated. Values equal to 3.17 ± 0.05 g cm^{-3} were obtained for both Al- and Ce-doped pellets, therefore confirming the constancy of the starting density for the different compositions.

The true strain $\varepsilon = \ln(l(t)/l_0)$, $l(t)$ being the instantaneous length as a function of time (t) and l_0 the initial length, determined upon sintering of the pellets is reported in Fig. 1. For all samples, when the dopant concentration increases from 1 to 5%, the curves shift to the right; this means that the higher the doping level, the slower is the sintering effect. This behaviour is more evident for the Ce-doped pellets, where the peak of the maximum sintering rate occurs at 1325, 1340 and 1355 °C for 1, 3 and 5% Ce-doped specimen, respectively. In addition, one can observe that the sintering curves of Al-doped pellets are shifted to the left if compared to the diagrams corresponding to Ce-doped samples at the same doping level.

Based on the above results, the two limit cases, corresponding to NiO doped with 1 mol% Al and 5 mol% Ce, were selected as starting anode precursor powders for further co-sintering analyses of the anode/electrolyte composite system.

Table 2
Specific surface area (SSA) of selected NiO powders.

	SSA (m^2 g^{-1})
As-received NiO	3.3
Calcined NiO	1.6
1 mol% Al–NiO	4.4
5 mol% Ce–NiO	4.1

Micrographs of the selected NiO powders are reported in Fig. 2. As received NiO powder looks coarser than doped one. The powders surface specific area (as measured by the nitrogen adsorption method) is reported in Table 2. One can consider an experimental error in SSA measurement of the order of 1 m^2 g^{-1}; on this basis, after Table 2, the heat treatment has the effect of coarsening pure NiO powder, thus decreasing SSA. Conversely, Al or Ce nitrate addition may have a twofold effect: first, it can limit NiO powder coarsening upon calcination; second, it may slightly increase the measured SSA since the oxides which are formed from the salts possess a very high specific surface area. Since the sintering behaviour depends also from the forming method [25], monolithic tapes were produced with the selected compositions in order to determine their sintering characteristics in the real condition. The anode green density was measured to be 2.48 ± 0.06 g cm^{-3}. The true strain and the shrinkage rate of the green tapes are reported in Fig. 3. The electrolyte is the fastest shrinking layer, with a maximum rate of 21.2×10^{-6} s^{-1} (absolute value) at 1340 °C. The Al-doped anode is the fastest sintering among the anodes, with a maximum rate of 13.7×10^{-6} s^{-1} at 1340 °C. A similar behaviour was observed both for Ce-doped and pure NiO anode. However, Ce-doped sample shows a slightly lower maximum rate at lower temperatures with respect to pure NiO anode (10.3×10^{-6} s^{-1} at 1375 °C and

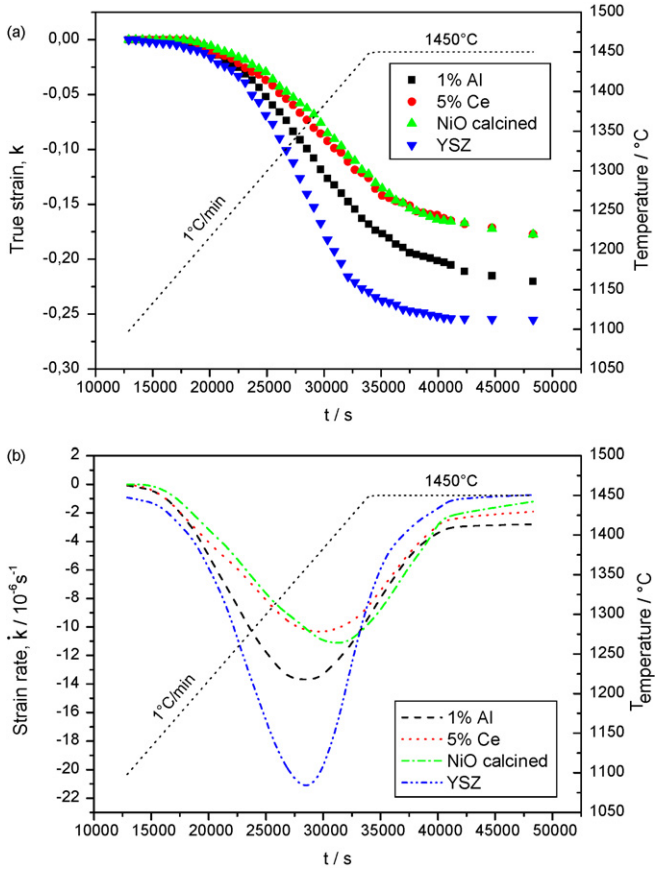

Fig. 3. True strain (a) and strain rate (b) as a function of time for tape cast layers.

$11.1 \times 10^{-6}\ s^{-1}$ at 1405 °C for Ce–NiO and NiO, respectively). The largest mismatch in sintering rate between anode and electrolyte is $11.0 \times 10^{-6}\ s^{-1}$ at 1340 °C for both Ce-doped and the undoped anode, while it is only $7 \times 10^{-6}\ s^{-1}$ at 1340 °C for the Al doped anode. The curves for the tape cast doped anodes confirm the trend already shown by the pressed pellet sintering curves: i.e. Al is more effective in accelerating the anode sintering compared to Ce. Though no data can be found in literature addressing the influence of Al or Ce on a NiO/YSZ composite sintering rate, consistently with the results found here it has been reported that Al_2O_3 is acting as a sintering aid for 8 mol% YSZ [14,15] while CeO_2 in concentration above 0.2% is decreasing the linear shrinkage rate in 3 mol% YSZ [26].

Three half cells were realised by casting the anode on a previously tape cast electrolyte and the curvature developed upon sintering was measured in situ. In order to minimise all possible errors, the three half cells were sintered in a single run; the developed normalised curvature $k = t/r$ (t being the layer thickness and r the radius of curvature) and the cell curvature rate are reported in Fig. 4. Fig. 5 shows a sequence of selected photographs of the three samples for clarifying the different behaviours. All cell are curving towards the electrolyte side in the firsts stages of sintering. Ce-doped and undoped cell start to curve around 1200 °C; Al-doped cell show initial deformation around 1250 °C. The normalised curvature continuously increases up to a maximum of 0.105 at 1420 °C, 0.095 at 1430 °C and 0.045 at 1390 °C, for the Ce doped, the undoped and the Al doped, respectively. After this peak, the curvature rate inverts its sign and the cells begin to curve towards the anode side. The maximum normalised curvature rate is $10.7 \times 10^{-6}\ s^{-1}$ at 1330 °C, $9.8 \times 10^{-6}\ s^{-1}$ at 1340 °C and $7.1 \times 10^{-6}\ s^{-1}$ at 1300 °C, for Ce-doped, undoped and Al-doped, respectively. It is worth noting

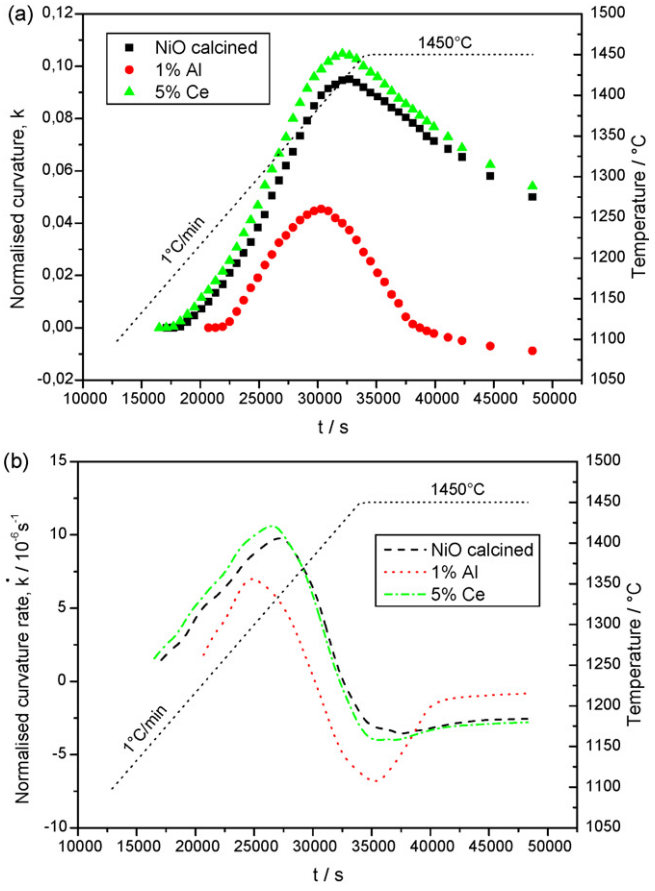

Fig. 4. Normalised curvature (a) and normalised curvature rate (b) of the half cells as a function of time.

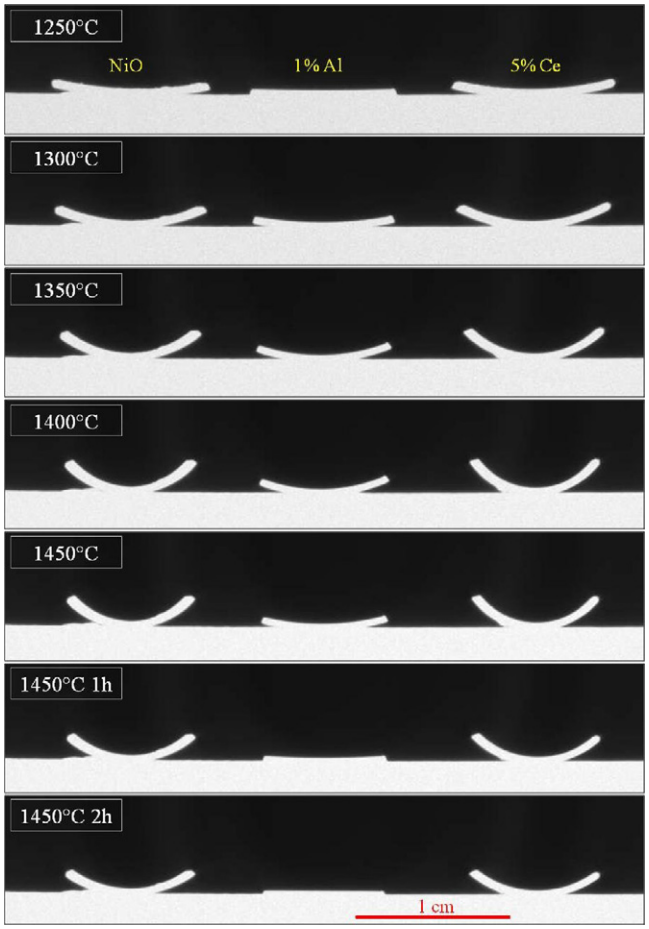

Fig. 5. Selected photographs of the half cells taken at different sintering times and temperatures. The samples are, from the left to the right: half cell produced with pure calcined NiO, 1 mol% Al-doped NiO and 5 mol% Ce-doped NiO. The electrolyte is the top layer.

that the only sample which totally recovers a flat configuration is the half cell with Al-doped anode, which is flat after an isotherm of 2 h at 1450 °C.

The obtained results are in good agreement with sintering rates data collected on monolithic layers: according to Cai et al. [1] the curvature rate of a bi-layer is proportional to the free sintering rate of the two layers. The samples considered here are in fact curving towards the electrolyte when the electrolyte free sintering rate is higher than the anode one, and vice versa. The temperature of curvature rate inversion corresponds with good approximation to the point where the anode begins to shrink faster than the electrolyte. The samples which are subjected to higher curvature rate are those where the mismatch sintering rate between anode and electrolyte is higher (i.e. the Ce-doped and the undoped one), while the Al-doped sample shows a lower curvature rate, the dopant having the effect of promoting sintering and, therefore, matching better its sintering rate with the electrolyte one.

The developed sintered microstructures are reported in Fig. 6. By examining the electrolyte surface and cross-section, one can notice that it is well densified in all samples and only closed porosity is present. The three anodes have retained enough porosity even before reduction to Ni. Nevertheless, only the electrolyte stacked to Al-doped anode is defect free. Signs of clear delamination between anode and electrolyte can be detected by examining the cross-section of Ce-doped and undoped sample and flaws are present on both electrolyte surfaces. The Ce-doped sample is the most severely damaged. It is worth to note that the defects could be detected

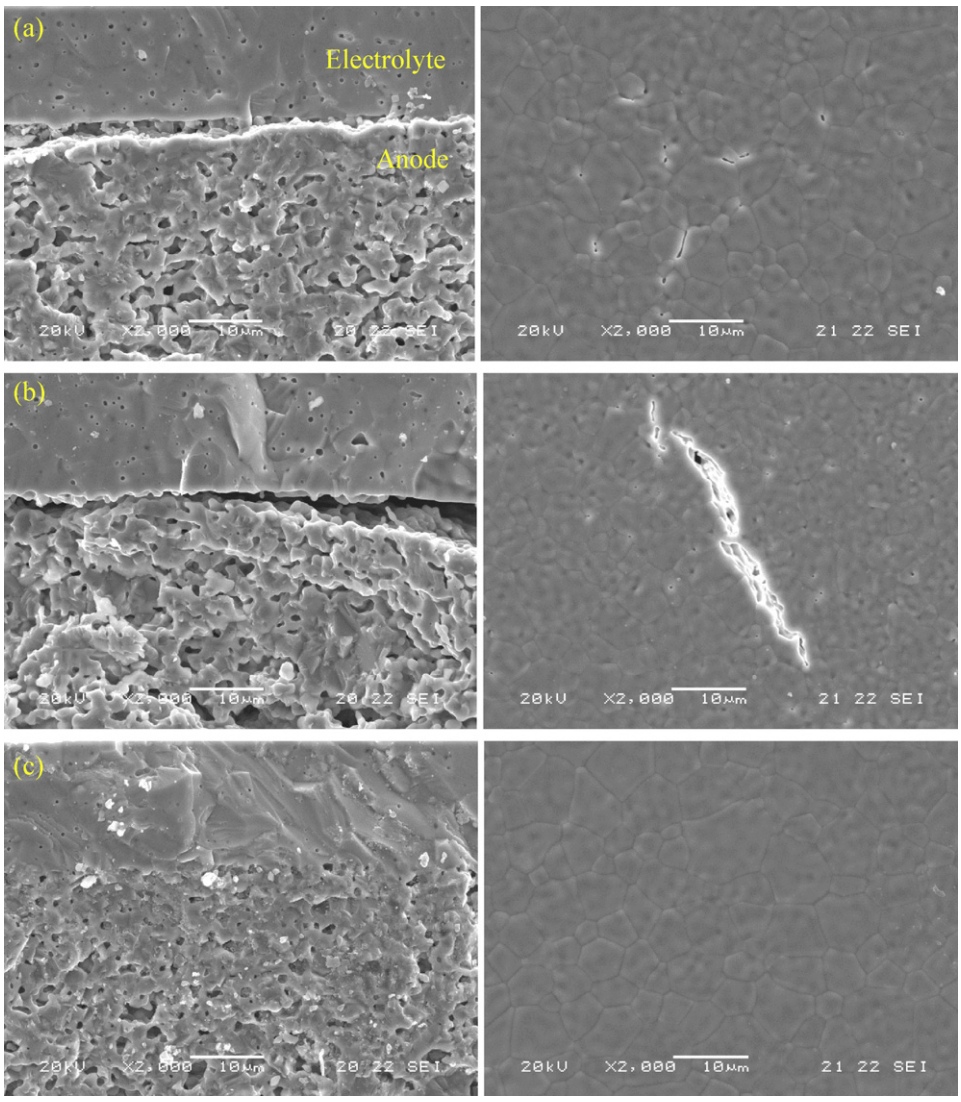

Fig. 6. Micrographs of the cross-section (on the left) and electrolyte surface (on the right) of the sintered half cells. Calcined NiO (a), 5 mol% Ce-doped NiO (b) and 1 mol% Al-doped NiO (c).

only with careful SEM examinations, since all cells were not visibly cracked and the electrolyte appeared smooth and translucent at a first examination even with an optical microscope.

The cracks observed on Ce-doped and in undoped sample are interpretable in terms of the free sintering rates data of the monolithic layers and are in good agreement with the measured curvature rates. In fact it has been previously reported that the stresses generated in the sintering of multilayered ceramics are proportional to the curvature rate (or to the mismatch sintering rate) [1]. The crack density on the electrolyte surface and their extension were found to be maximum in the cell that reaches the maximum curvature rate. Flaws or de-bonding defects similar to those reported here have been found in alumina/zirconia laminates [1] and in tape cast layers sintering under an applied load [27] and were thought to originate in the sintering stage, when the stresses (applied externally or originated internally) exceed the layer strength. Nevertheless, the determination of the exact moment for crack development is not straightforward: the developed stresses and the strength of the layers are continuously changing during sintering, being them dependent on other factors like temperature, density and grain size. It is however likely that such cracks initiate in the first and intermediate stages of sintering, when the layers strength is still low and the mismatch sintering rate is higher. Even if an exact quantification of the stresses and of the ceramic compact strength requires the knowledge of the mechanical response of the ceramic sintering compact in every instant of densification, it can be foreseen that NiO/YSZ anode precursor layer possessing sintering rate curve between that shown by Al-doped anode and by the electrolyte, will be successfully co-fired with the electrolyte without cracks development.

Polarisation curves for cells produced with 1 mol% Al- and 5 mol% Ce-doped NiO and undoped NiO are reported in Fig. 7. The aluminium containing cell shows an open circuit voltage (OCV) of 1054 mV and a power density at 0.7 V of 579 mW cm^{-2} at 800 °C. At the same temperature, the cerium containing cell possesses an OCV of 960 mV and a power density at 0.7 V of 368 mW cm^{-2}. The cell produced using pure NiO shows an OCV of 1055 mV and power density at 0.7 V of 241 mW cm^{-2}. The high OCV of the Al-doped NiO containing cell is a direct consequence of the gas tightness of the electrolyte in agreement with previous microstructural observations (Fig. 6c). The lower power densities measured for both Ce-doped and undoped NiO containing cells can probably be ascribed to the presence of defects mainly consisting of delaminating flaws which occur at the anode/electrolyte interface during the sintering process. The relatively limited OCV measured for the Ce-doped cell can be accounted for the presence of severe flaws within

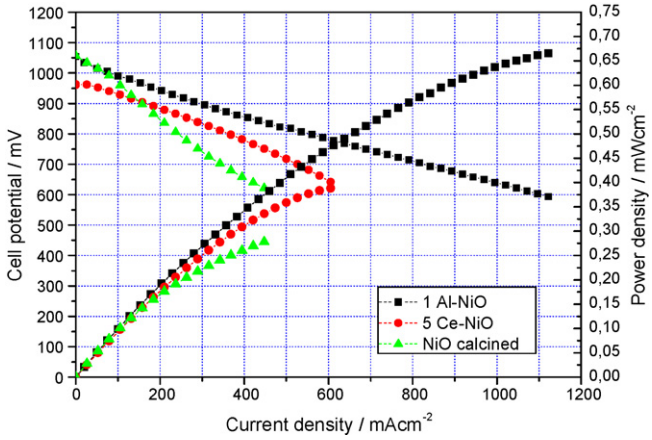

Fig. 7. Polarisation curves at 800 °C for the cells produced with 1 mol% Al-, 5 mol% Ce-doped NiO and undoped NiO.

the electrolyte as shown in Fig. 6b. Conversely, the electrolyte of the cell made by pure NiO is less severely damaged, this being reflected by a still high OCV value.

4. Conclusions

The influence of Al and Ce on sintering process of NiO/YSZ based anodes and on cell curvature developed upon co-firing was investigated.

The present work demonstrates how even a small addition of doping element can vary sensibly the sintering behaviour of SOFCs, thus being decisive in the successful production or failure of the device. In addition, the anode features cannot be simply modified by foreign element addition in the green state, because special care has to be addressed also to the effect this may have on the delicate issue of co-sintering with the electrolyte. Conversely, the use of reactive elements, if carefully controlled, can be successfully employed to tailor the anode sintering curve, to reduce the mismatch sintering rate with the electrolyte and allow the attainment of flat and high quality cells.

More in detail, Al is shown to increase the anode sintering rate; the cell assembled with Al-doped NiO powders shows lower curvature rate and is perfectly flat at the end of the sintering cycle. The curvature rate and the number of defects are higher for the sample having larger mismatch sintering rate between anode and electrolyte.

High quality cells that show low curvature rates and are flat at the end of the sintering process can be obtained starting from 1 mol% Al-doped NiO powders. Microstructural observation confirms the absence of defects in the produced cells that result in high performances upon electrochemical tests.

Acknowledgements

Authors thank Dr. Stefano Modena and Dr. Sergio Ceschini (SOFCpower S.r.l.) for their help in the electrochemical characterization.

References

[1] P.Z. Cai, G.L. Messing, D.L. Green, J. Am. Ceram. Soc. 80 (1997) 1929–1939.
[2] P.Z. Cai, G.L. Messing, D.L. Green, J. Am. Ceram. Soc. 80 (1997) 1940–1948.
[3] D.J. Green, O. Guillon, J. Rödel, J. Eur. Ceram. Soc. 28 (2008) 1451–1466.
[4] W. Li, K. Hasinska, M. Seabaugh, S. Swartz, J. Lannutti, J. Power Sources 138 (2004) 145–155.
[5] Y.J. Leng, S.H. Chan, K.A. Khor, S.P. Jiang, P. Cheang, J. Power Sources 117 (2003) 26–34.
[6] T. Garino, Ceram. Eng. Sci. Proc. 23 (2002) 759–766.
[7] S.P. Jiang, S.H. Chan, J. Mater. Sci. 39 (2004) 4405–4439.
[8] L. Jia, Z. Lub, J. Miaob, Z. Liu, G. Li, W. Sua, J. Alloys Compd. 414 (2006) 152–157.
[9] S. Primdahl, B.F. Sørensen, M. Mogensen, J. Am. Ceram. Soc. 83 (2000) 489–494.
[10] D. Donga, M. Liu, Y. Donga, B. Lin, J. Yang, G. Menga, J. Power Sources 171 (2007) 495–498.
[11] K.C. Wincewicz, J.S. Cooper, J. Power Sources 140 (2005) 280–296.
[12] E. Ivers-Tiffe'e, A. Weber, D. Herbstritt, J. Eur. Ceram. Soc. 21 (2001) 1805–1811.
[13] W.Z. Zhu, S.C. Deevi, Mater. Sci. Eng. A 362 (2003) 228–239.
[14] S. Tekeli, Mater. Des. 28 (2007) 713–716.
[15] A.A.E. Hassan, N.H. Menzler, G. Blass, M.E. Ali, H.P. Buchkremer, D. Stöver, J. Mater. Sci. 37 (2002) 3467–3475.
[16] S. Tekeli, Compos. Sci. Technol. 65 (2005) 967–972.
[17] W.G. Wang, W.B. Guan, H.M. Li, Y.J. Xue, J.X. Wang, Y.N. Wu, J. Wang, K. Liu, Proceedings of the 8th European Solid Oxide Fuel Cell Forum, Lucerne, CH, 30 June–4 July, 2008.
[18] P.H. Larsen, C. Chung, M. Mogensen, Redox-stable anode, WO Patent 2006079558.
[19] C.M. Finnerty, N.J. Coe, R.H. Cunningham, R.M. Ormerod, Catal. Today 46 (1998) 137–145.
[20] T. Takeguchia, R. Kikuchia, T. Yanoa, K. Eguchi, K. Murata, Catal. Today 84 (2003) 217–222.
[21] N. Nakagawa, H. Sagara, K. Kato, J. Power Sources 92 (2001) 88–94.
[22] J. Qiao, K. Suna, N. Zhang, B. Suna, J. Kong, D. Zhoua, J. Power Sources 169 (2007) 253–258.
[23] S. Modena, S. Ceschini, D. Montinaro, M. Bertoldi, Development and characterization of doped ceria buffer layers, in: Proceedings of the 8th European Solid Oxide Fuel Cell Forum, Lucerne, CH, 30 June–4 July, 2008.
[24] D. Ravi, D.J. Green, J. Eur. Ceram. Soc. 26 (2006) 17–25.
[25] O. Guillon, J. Rödel, R.K. Bordia, J. Am. Ceram. Soc. 90 (2007) 1637–1640.
[26] G. Yan, Z. Fu Quiang, H. Hui, Z. Yuan Li, L. Ying, J. Ceram. Process. Res. 9 (2008) 311–316.
[27] V.M. Sglavo, P.Z. Cai, D.J. Green, J. Mater. Sci. Lett. 18 (1999) 895–900.